

## Electric-field-induced anti-Stokes photoluminescence in an asymmetric GaAs/(Al,Ga)As double quantum well superlattice

L. Schrottke, R. Hey, and H. T. Grahn

*Paul-Drude-Institut für Festkörperelektronik, Hausvogteiplatz 5–7, D-10117 Berlin, Germany*

(Received 26 May 1999)

We have used photoluminescence (PL) spectroscopy to study the population properties of an asymmetric GaAs/(Al,Ga)As double quantum well superlattice, which represents a simplified version of the active region of a quantum cascade laser. The investigation focuses on the anti-Stokes PL signal of the narrower well, which is observed for excitation between the excitonic states of the two quantum wells and sufficiently high electric field strengths. In this case, the photocarriers are only excited in one of the two wells, and the signal gives direct evidence for transport of electrons *and* holes through the (Al,Ga)As barriers. An analysis of the electric-field dependence of conventional PL as well as anti-Stokes PL demonstrates that population inhomogeneities for the electronic states can be determined. [S0163-1829(99)16547-0]

Since the first proposal by Kazarinov and Suris in 1971,<sup>1</sup> considerable efforts have been made to utilize intersubband emission in semiconductor superlattice structures for infrared lasers in the 3–5- $\mu\text{m}$  as well as the 8–13- $\mu\text{m}$  atmospheric windows. These wavelength regions are important for a variety of applications, e.g., environmental sensing and process controlling. However, the first operating lasers were not reported until 1994 by Faist *et al.* for the (Ga,In)As/(Al,In)As system [quantum cascade laser<sup>2</sup> (QCL)] and 1997 by Lin *et al.* for the InAs/(In,Ga)Sb/AlSb system (interband cascade laser).<sup>3</sup> At the same time, optically pumped infrared laser action was demonstrated using simple asymmetric coupled quantum wells.<sup>4</sup> In addition to their great practical interest, the cascade structures also deserve attention for their basic physical properties.

Photoluminescence (PL) spectroscopy seems to be an appropriate tool to investigate the population of subband states in such structures,<sup>5,6</sup> although the excitation of electron-hole pairs is not compatible with the unipolar character of the QCL. In quantum well (QW) structures with different well thicknesses, i.e., in which the excitonic states are both energetically and spatially separated from each other, two excitation conditions are of particular importance. In conventional PL experiments, the excitation energy is well above all relevant transition energies so that electron-hole pairs are created in all QW's. In an electric field, the electrons and/or holes can be redistributed by transport processes. For an excitation energy between the excitonic states of the QW's, electrons and holes are only excited in the wider wells so that any PL signal from the narrower QW's would give direct evidence of the transport of electrons *and* holes through the barriers. This type of PL signal appears at a higher photon energy than the excitation energy and is therefore referred to as anti-Stokes PL. In contrast to the reported low-temperature anti-Stokes PL signals in the literature,<sup>7–11</sup> an electric field is required, which has to be sufficiently strong to allow the transport of electrons as well as holes from the wider to the narrower wells. Therefore, this anti-Stokes PL induced by the applied electric field is expected to exhibit a threshold behavior.

In this paper, we investigate the population properties of

an asymmetric GaAs/(Al,Ga)As double quantum well superlattice, which represents a simplified active region of a QCL, using anti-Stokes as well as conventional PL spectroscopy. The PL spectra were recorded as a function of the applied electric field for different excitation energies and field polarities. We demonstrate that the electronic transport behavior results in a population inhomogeneity between the two quantum-well electronic ground states and that PL spectroscopy can be applied as a simple measuring technique to characterize the underlying processes. An estimation of the population ratio between the ground states of adjacent wells from the electric-field dependence of the PL signal is also presented.

The samples consist of a superlattice structure with a unit cell containing two wells and two barriers, which all have different thicknesses. The unit cell is shown schematically in Fig. 1, where  $d_1^w$  ( $d_1^b$ ) and  $d_2^w$  ( $d_2^b$ ) denote the thickness of the wider and narrower well (barrier), respectively. While the barriers of different thickness result in different transfer rates, which are expected to lead to an occupation inhomogeneity or even a possible population inversion between the electronic ground states of the adjacent wells, the difference in the well widths leads to different transition energies for the two QW's. Therefore, the QW's following the thick barrier (with respect to the direction of the electric field) can be distinguished from the ones following the thin barrier through their respective PL energy. Due to the asymmetry of

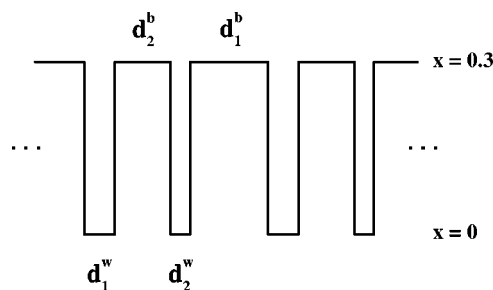


FIG. 1. Schematic diagram of the Al mole fraction for two unit cells of the asymmetric GaAs/Al<sub>x</sub>Ga<sub>1-x</sub>As double quantum well superlattice.

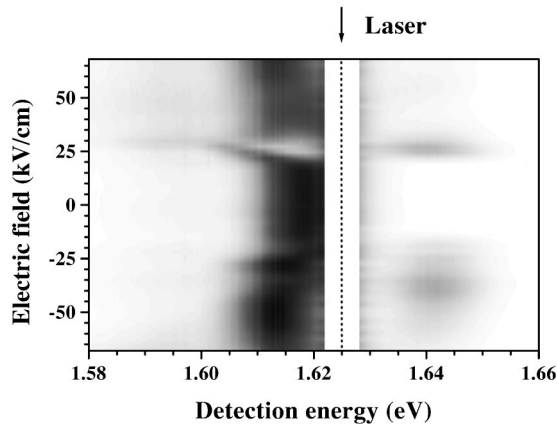


FIG. 2. PL intensity as a function of detection energy and applied electric field measured at a temperature of 5 K for an excitation energy between the excitonic states of the two quantum wells as indicated by the dashed line. Darker areas correspond to high intensities, lighter areas to low intensities.

the unit cell, forward and reverse bias refer to different injection conditions. We define forward bias as the polarity for which the electron ground state of the wider well is at a higher potential than the one of the adjacent narrower well, if they are connected by the thin barrier. The opposite polarity is referred to as reverse bias, i.e., the same situation as above except that the thick barriers are now connecting the two wells. In the schematic diagram of Fig. 1, forward bias corresponds to the situation, where the left-hand side is at a higher potential. In this paper, forward bias is represented by a positive electric-field strength.

The  $\text{Al}_{0.3}\text{Ga}_{0.7}\text{As}/\text{GaAs}$  superlattice structure, which forms the intrinsic region of an  $n^+i-n^+$  diode, was grown by molecular-beam epitaxy on an  $n^+$ -GaAs substrate. It contains 20 periods with the following parameters,  $d_1^w=5$ ,  $d_2^w=4$ ,  $d_1^b=14$ , and  $d_2^b=10$  nm. Between the doped layers and the 20-period structure, a 25-nm GaAs well, a 10-nm  $\text{Al}_{0.3}\text{Ga}_{0.7}\text{As}$  barrier, and a 5-nm GaAs well are inserted on the substrate side and a 10-nm  $\text{Al}_{0.3}\text{Ga}_{0.7}\text{As}$  barrier as well as another 25-nm GaAs well on the top side so that the intrinsic region has a total thickness of 735 nm. The  $n^+$ -layers consist of Si-doped GaAs with a doping density of  $2 \times 10^{18} \text{ cm}^{-3}$  and compositionally graded, Si-doped  $\text{Al}_x\text{Ga}_{1-x}\text{As}$  optical window layers. The sample is processed into mesas of 210- $\mu\text{m}$  diameter with AuGe/Ni contacts of 70- $\mu\text{m}$  diameter, which are small enough for optical access to the structure through the top contact. For the PL experiments, the sample was mounted on the cold finger of a He-flow cryostat. The optical excitation was carried out with an  $\text{Ar}^+$ -laser-pumped Ti:sapphire laser tuned to the excitation energies of 1.625 and 1.722 eV. The PL signal was dispersed in a 1-m monochromator and detected with a cooled charge-coupled-device detector. The laser power was adjusted to about 50 nW with the beam focused to a diameter of about 100  $\mu\text{m}$ .

Figure 2 shows the observed PL intensity as a function of detection energy and electric field in a gray-scale representation for an excitation energy between the excitonic states of the two QW's. The rather intense stray light from the laser, which is reflected diffusely at the surface of the sample, has been covered by the white area. The energetic position of the

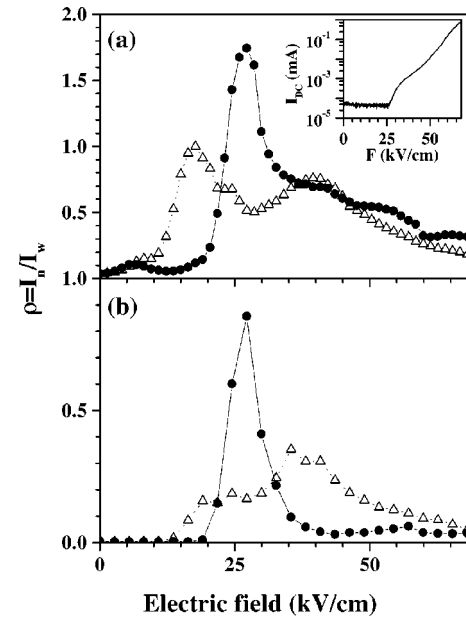


FIG. 3. Ratio  $\rho = I_n/I_w$  of the integrated PL intensities of the narrower ( $I_n$ ) and wider ( $I_w$ ) QW's for excitation energies of (a) 1.722 and (b) 1.625 eV vs applied electric field for forward (dots) and reverse bias (triangles). In (b),  $\rho$  corresponds to the ratio of the anti-Stokes to the Stokes PL intensity. The inset of (a) represents the current-voltage characteristic, i.e., dc current ( $I_{DC}$ ) as a function of electric field ( $F$ ), without laser excitation.

laser of 1.625 eV is marked by the dashed line. The Stokes PL line has its maximum at 1.615 eV with a rather constant intensity over the whole field range except for a field near +27 kV/cm, where it exhibits a well-defined minimum. Furthermore, an additional (diagonal) transition between the adjacent wells is observed, which exhibits an energy shift almost linearly dependent on the electric field. The anti-Stokes PL at 1.642 eV is observed for a field strength of about +27 kV/cm as well as between  $-15$  and  $-70$  kV/cm.

In order to have an experimental quantity that is related to the occupation of the quantum well states, we define the ratio  $\rho = I_n/I_w$  of the integrated PL intensity  $I_n$  of the narrower and  $I_w$  of the wider well, which is shown in Figs. 3(a) and 3(b) as a function of the applied electric field strength for excitation above and below the ground state of the narrower well, respectively. For both excitation conditions and forward bias,  $\rho$  exhibits a clear maximum near 27 kV/cm. Another smaller maximum exists for excitation of both quantum wells near 5 kV/cm. In reverse bias,  $\rho$  appears to have two maxima for both excitation conditions. An increase of the excitation intensity, i.e., carrier density, by two orders of magnitude leads only to a reduction of the maximum value of  $\rho$  for forward bias, but does not shift the features of the  $\rho$ -curves with respect to the field strength. Therefore, the carrier concentration is sufficiently small in order to neglect band-bending effects for field strengths below about 30 kV/cm.

According to the solution of the Schrödinger equation in the envelope function approximation, several characteristic field strengths exist, at which electron or heavy-hole states of two adjacent wells are at the same energy. Let us focus on the forward bias condition. Below 4.6 kV/cm, the electron as well as the hole states form a ripplelike sequence of upward

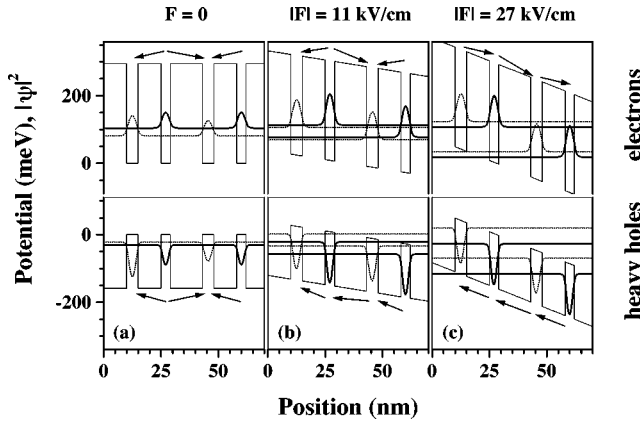


FIG. 4. Calculated electron and heavy-hole states within the multiple QW system for different electric field strengths: (a) 0, (b) 11, and (c) 27 kV/cm (corresponding to voltages of 0, 0.80, and 1.95 V, respectively, using a total thickness of the intrinsic region of 735 nm) for forward bias as defined in the text. The arrows indicate the direction of a possible transfer of the carriers.

and downward steps as shown in Fig. 4(a) for forward bias so that both types of carriers can only move from the narrower to the wider wells, if the narrower-well states are occupied. At 4.6 kV/cm, the heavy-hole states of the adjacent wells become resonantly aligned, and the transfer from the narrower to the wider well via the thick barrier becomes possible. The next characteristic field strength is 16 kV/cm, at which the electron states of adjacent wells are in resonance via the thin barrier. Between 4.6 and 16 kV/cm, the electron states remain in the ripplelike structure, while the heavy-hole states form already a ladder as shown in Fig. 4(b) for 11 kV/cm. In this field region, field-induced transport of heavy holes from the wider to the narrower well becomes possible via the thick barrier, while the electrons cannot move from the wider to the narrower well via the thin barrier yet. For field strengths above 16 kV/cm [cf. Fig. 4(c) for 27 kV/cm], both electron as well as heavy-hole states form a ladder.

These characteristic field strengths can be correlated with significant points in the experimental  $\rho$  curves as shown in Figs. 3(a) and 3(b). For excitation above the ground state of the narrower wells [cf. Fig. 3(a)] and forward bias, the first maximum of  $\rho$  at about 5 kV/cm coincides with the first heavy-hole resonance. Above 16 kV/cm,  $\rho$  strongly increases due to the increased electron transfer from the wider to the narrower well through the thin barrier. The field dependence of  $\rho$  exhibits in this regime an onsetlike behavior. Since the PL intensity, and hence  $\rho$ , is proportional to the product of electron and hole concentration for each QW, the field dependence of  $\rho$  does not directly reflect the occupation of electron or hole states alone. Surprisingly, the PL signal of the narrower well due to direct occupation by photoexcitation is rather small below 5 kV/cm. This low value of  $\rho$  provides evidence of a rather strong transfer of electrons as well as holes from the narrower wells to the lower states in the wider wells. Above 5 kV/cm, the preferred hole transport occurs through the thin barrier from the narrower to the wider well so that  $\rho$  exhibits a minimum just below the resonance condition for electrons at 16 kV/cm. Above this field strength,  $\rho$  exhibits a strong increase, since the electrons dominate the carrier transport for these field strengths. The

second maximum of  $\rho$  at 27 kV/cm is probably related to the dramatic increase of the current above 2 V (27 kV/cm) as shown in the inset of Fig. 3(a). This high current may lead to a different transfer mechanism through the barriers, e.g., activation by electron impact excitation. Therefore, the electron transfer rates to the narrower well becomes similar to the transfer to the wider wells, although the carriers have to pass through differently thick barriers. The weaker structures at higher electric fields are beyond the scope of this paper.

Within a very simple rate equation model for a unipolar system, i.e., only electrons are considered, one expects that the occupation ratio  $\eta = n_n/n_w$  of the electronic subband states of adjacent wells is proportional to the ratio  $t_{wn}/t_{nw}$  with  $t_{wn}$  and  $t_{nw}$  denoting the transfer rates from the wider to the narrower well and vice versa, respectively. However, probing  $\eta$  with PL spectroscopy requires to include the hole distribution into the model, which results in a nonlinear system of partial differential equations. Since there are too many variables in this case, it does not allow to derive reasonable conclusions on the absolute values of the rates from this experiment alone. In order to achieve at least a qualitative discussion, the hole concentrations are included into the electronic model by modifying the recombination terms, so that they are proportional to  $n$  only. Then, the ‘‘combined’’ recombination rates  $r_w$  and  $r_n$  for the two wells are proportional to the hole concentrations, but are considered to be approximately independent of the electronic system. We obtain

$$\rho \sim \frac{1 + 2t_{wn}/r_w}{1 + 2t_{nw}/r_n} = \frac{r_n/t_{nw}}{2 + r_n/t_{nw}} + \frac{2}{2 + r_n/t_{nw}} \nu, \quad (1)$$

with

$$\nu = \left( \frac{t_{wn}}{t_{nw}} \right) \left( \frac{r_n}{r_w} \right). \quad (2)$$

The right-hand side demonstrates that  $\rho$  is a linear function of  $\nu$ , if the term  $r_n/t_{nw}$  is assumed to be constant. The influence of this term itself is, however, not straight forward. Figure 5 shows  $\rho$  as a function of  $r_n/t_{nw}$  for several values of  $\nu$ . While in the limit of very low hole concentration, i.e.  $r_n \ll t_{nw}$ , which corresponds in our experiment to a very low excitation intensity, the measured value  $\rho$  is close to the value of  $\nu$ , it tends to unity for higher excitation intensity. In this situation, the peak value at 27 kV/cm may be considered as a result of the (larger) transfer rate into the narrow well through the thinner barrier so that it can become larger than one. The excitation intensity dependence of the measured values of  $\rho$ , which are included as symbols in Fig. 5 agrees well with the calculated dependence of  $\rho$  on  $r_n/t_{nw}$ . The only fitting parameter is the scaling between the excitation power and  $r_n/t_{nw}$ . The best agreement is achieved, when  $r_n = t_{nw}$  for 0.5  $\mu$ W. For very low ( $< 5$  nW) and very high excitation powers ( $> 50$   $\mu$ W), the measured value is lower than the calculated one. At low power, the diagonal transition (cf. Fig. 2) as well as noise is relatively strong so that the determination of  $\rho$  from the spectra becomes increasingly uncertain, while at high excitation intensities, saturation effects play probably an important role.

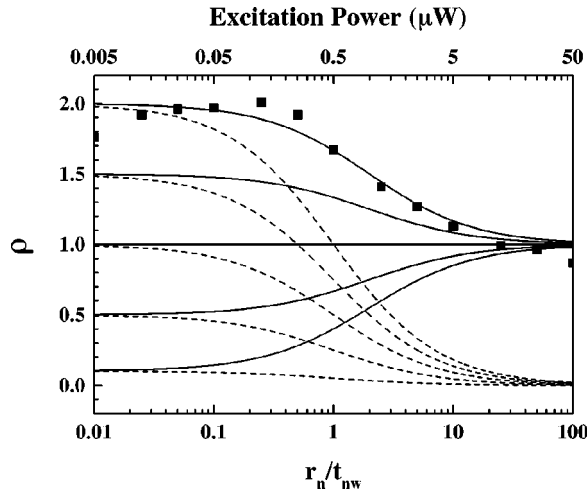


FIG. 5. Calculated values of  $\rho$  as a function of  $r_n/t_{nw}$  according to Eq. (1) for several values of  $\nu$  (0.1, 0.5, 1, 1.5, 2) for excitation in both QW's (solid) and in the wide QW's alone (dashed). The experimental values of  $\rho$  for an electric field strength of 27 kV/cm and excitation in both wells as a function of excitation intensity are inserted as solid squares.

For excitation below the ground state of the narrower well as shown in Fig. 3(b), i.e.,  $g_n=0$  and  $g_w=g$ , Eq. (1) is modified to

$$\rho \sim \frac{t_{wn}/r_w}{1+t_{nw}/r_n} = \frac{1}{1+r_n/t_{nw}} \nu. \quad (3)$$

In this case,  $\rho$  is directly proportional to  $\nu$ . Furthermore,  $\rho$  is considerably smaller for not too low intensities (cf. Fig. 5), which is in good agreement with the experimental result, i.e., the maximum value at 27 kV/cm is about a factor of 2 smaller than for excitation in both QW's. Any increase of  $r_n/t_{nw}$ , either by an increase of  $r_n$  or an decrease of  $t_{nw}$ , leads to a strong decrease of  $\rho$ , as shown in Fig. 5 (anti-Stokes case).

For reverse bias, the characteristic field strength of the hole resonance is slightly larger (5.4 kV/cm), since the coupling occurs through the thin barrier. However, the field strength of the electron resonance amounts to a smaller value (13 kV/cm), since in this case the wide and narrow well are coupled through the wider barrier. At 30 kV/cm, the ground and first excited heavy-hole states are in resonance via the thick barrier. The measured field dependencies of  $\rho$  for the two polarities differ significantly. In reverse bias, the population of the electron states of the narrower well is expected to be smaller compared to the case of forward bias, since the coupling of the electron states occurs now through the thick barriers. The opposite polarity behavior is expected for the heavy-hole states, since the current flow direction is reversed. In contrast to forward bias, the increase in  $\rho$  related to the electron resonance occurs at much smaller field strengths. This may be an indication that the transfer of holes into the narrower wells through the thin barriers is comparatively strong so that the maximum of the PL intensity is probably directly connected with the electron resonance at about 13 kV/cm. For higher field strengths at reverse bias, the nonresonant tunneling of electrons leads to an increase of the occupation of the wider wells. Due to the above men-

tioned different transfer mechanism, the sharp decrease of  $\rho$  at 27 kV/cm for forward bias corresponds to a respective increase for reverse bias. Finally, in the case of photoexcitation in both wells, the  $\rho$  curves are equal for the two polarities above 35 kV/cm. The different behavior in the anti-Stokes case, at which  $\rho$  is considerably larger for reverse bias than for forward bias, can qualitatively be explained with the help of Eq. (3). Assuming  $t_{nw} \approx t_{wn}$ ,  $\rho$  is mainly determined by the hole density, i.e., the recombination rate  $r_n$  for the narrow wells, which is much smaller for forward than for reverse bias, while  $r_w$  may be assumed to be similar for both polarities.

Despite these complex transport properties, the occupation ratio  $\eta$  can be estimated for field strengths above the electron resonances, at which the investigated structure simulates the behavior of the active region of a QCL. The intensity ratios for forward and reverse bias  $\rho^f$  and  $\rho^r$ , respectively, are proportional to  $\eta^{f,r}$

$$\rho^{f,r} = CR^{f,r} \eta^{f,r} \quad (4)$$

with the proportionality factors  $R^{f,r} = r_n^{f,r}/r_w^{f,r}$  and  $C$ . The constant  $C$  reflects the spectral properties of the sample and the detector independently of the polarity. Insofar as it is only the barrier thicknesses (and not the different energetic positions of the electron and hole states in the wells) that determine the transport properties, we may assume for further simplification that  $\eta^f = 1/\eta^r = \eta$ , which seems to be reasonable for sufficiently high field strengths, so that  $C$  can be eliminated resulting in

$$\eta = \sqrt{\frac{\rho^f}{\rho^r}} \sqrt{\frac{R^r}{R^f}}. \quad (5)$$

Furthermore, since the electrons dominate the transport of carriers at higher field strengths, the second factor in this equation may be assumed to be about 1 for conventional PL, so that the approximate value of  $\eta$  can directly be calculated from the  $\rho$  curves shown in Fig. 3(a). At its maximum,  $\eta$  reaches a value of 1.8. Note, however, that a precise quantitative discussion would require a detailed numerical analysis taking into account the (electric-field-dependent) transfer rates of electron and heavy-holes states through the different barriers as well as possible field inhomogeneities.

In summary, this investigation demonstrates that PL and in particular anti-Stokes PL spectroscopy of asymmetric double quantum well superlattices can be used for a qualitative discussion of the occupation properties of the quantum well states. Characteristic field strengths of the structure can be correlated with extrema in the field dependence of the relative intensity of the two quantum wells. Although the anti-Stokes PL gives direct evidence that both electrons and holes participate in the transport processes, a strong electric-field dependent population inhomogeneity was demonstrated for the case of low excitation intensities. Furthermore, anti-Stokes PL seems to be a very useful tool to investigate carrier transfer in such structures.

- <sup>1</sup>R. F. Kazarinov and R. A. Suris, *Fiz. Tekh. Poluprov.* **5**, 797 (1971) [*Sov. Phys. Semicond.* **5**, 707 (1971)].
- <sup>2</sup>J. Faist, F. Capasso, D. L. Sivco, C. Sirtori, A. L. Hutchinson, and A. Y. Cho, *Science* **264**, 553 (1994).
- <sup>3</sup>C.-H. Lin, R. Q. Yang, D. Zhang, S. J. Murry, S. S. Pei, A. A. Allerman, and S. R. Kurtz, *Electron. Lett.* **33**, 598 (1997).
- <sup>4</sup>O. Gauthier-Lafaye, P. Boucaud, F. H. Julien, S. Sauvage, S. Cabaret, J.-M. Lourtioz, V. Thierry-Mieg, and R. Planel, *Appl. Phys. Lett.* **71**, 3619 (1997).
- <sup>5</sup>H. T. Grahn, H. Schneider, W. W. Rühle, K. v. Klitzing, and K. Ploog, *Phys. Rev. Lett.* **64**, 2426 (1990).
- <sup>6</sup>Y. B. Li, J. W. Cockburn, J. P. Duck, M. J. Birkett, M. S. Skolnick, I. A. Larkin, M. Hopkinson, R. Grey, and G. Hill, *Phys. Rev. B* **57**, 6290 (1998).
- <sup>7</sup>E. J. Johnson, J. Kafalas, R. W. Davies, and W. A. Dyes, *Appl. Phys. Lett.* **40**, 993 (1982).
- <sup>8</sup>Y. Mori, K. Onozawa, H. Ohkura, and Y. Chiba, *J. Lumin.* **48&49**, 800 (1991).
- <sup>9</sup>R. Hellmann, A. Euteneuer, S. G. Hense, J. Feldmann, P. Thomas, E. O. Göbel, D. R. Yakovlev, A. Waag, and G. Landwehr, *Phys. Rev. B* **51**, 18 053 (1995).
- <sup>10</sup>D. S. Kim *et al.*, *Prog. Cryst. Growth Charact.* **33**, 161 (1996).
- <sup>11</sup>L. Schrottke, H. T. Grahn, and K. Fujiwara, *Phys. Rev. B* **56**, R15 553 (1997).